Dynamic Functional Hyperconnectivity after Psilocybin Intake is Primarily Associated with Oceanic Boundlessness

Sepehr Mortaheb[1,2±], Larry D. Fort[1,2±], Natasha L. Mason[3], Pablo Mallaroni[3], Johannes G. Ramaekers[3*±], Athena Demertzi[1,2,4*±]

[1]Physiology of Cognition, GIGA-CRC In Vivo Imaging, University of Liège, Belgium

[2]Fund for Scientific Research FNRS, Brussels, Belgium

[3]Department of Neuropsychology and Psychopharmacology, Faculty of Psychology and Neuroscience, Maastricht University, The Netherlands

[4]Psychology & Neuroscience of Cognition (PsyNCog), University of Liège, Belgium

[±]Equal contribution

[*]Corresponding authors:

a.demertzi@uliege.be

j.ramaekers@maastrichtuniversity.nl

Abstract

To provide insights into neurophenomenological richness after psilocybin intake, we investigated the link between dynamical brain patterns and the ensuing phenomenological pattern after psilocybin intake. Healthy participants received either psilocybin (n=22) or placebo (n=27) while in ultra-high field 7T MRI scanning. Changes in the phenomenological patterns were quantified using the 5-Dimensional Altered States of Consciousness (5D-ASC) Rating Scale, revealing alterations across all dimensions under psilocybin. Changes in the neurobiological patterns displayed that psilocybin induced widespread increases in averaged functional connectivity. Time-varying connectivity analysis unveiled a recurrent hyperconnected pattern characterized by low BOLD signal amplitude, suggesting heightened cortical arousal. In terms of neurophenomenology, canonical correlation analysis primarily linked the transition probabilities of the hyperconnected pattern with feelings of oceanic boundlessness (OBN), and secondly with visionary restructuralization. We suggest that the brain's tendency to enter a hyperconnected-hyperarousal pattern under psilocybin represents the potential to entertain variant mental associations. For the first time, these findings link brain dynamics with phenomenological alterations, providing new insights into the neurophenomenology and neurophysiology of the psychedelic state.

Introduction

Hallucinogens are psychoactive drugs that, historically, have been used to alter conscious experience[1,2]. These drugs are divided into the classes of serotonergic psychedelics (e.g., psilocybin), antiglutamatergic dissociatives (e.g., ketamine), anticholinergic deliriants (e.g., scopolamine) and kappa-opioid agonists (e.g., salvinorin A)[3]. Research on classical hallucinogens has focused largely on serotonergic psychedelics, such as lysergic acid diethylamide (LSD), ayahuasca, psilocybin, N-dimethyltryptamine (DMT), and mescaline[4]. Among them, psilocybin has been one of the most studied psychedelics, possibly due to its potential contribution in treating different disorders[5], such as obsessive-compulsive disorder[6], death-related anxiety[7], depression[8–11], treatment-resistant depression[12–14], major depressive disorder[15], terminal cancer-associated anxiety[11,16], demoralization[17], smoking [18], and alcohol and tobacco addiction[19–21].

The acute phase of psilocybin administration leads to the psychedelic state, which is a specific altered state of consciousness associated with consuming psilocybin and LSD[22]. By "state" we here refer to the combination of neurobiological and phenomenological patterns that are associated with the psychedelic experience.[24] In terms of the general phenomenological pattern, the psychedelic state has been associated with the experience of ego dissolution (i.e., the reduction in self-referential awareness, ultimately disrupting self-world boundaries with increasing feelings of unity with others and own surroundings)[25,26], unconstrained and hyper-associative cognition[27,28], profound alterations in the perception of time, space and selfhood[29,30], perceptual alterations, synesthesia, amplification of emotional state[31], and emotional volatility[32]. Long-term and enduring effects have also been reported on personality and mood, such as increases in openness and extraversion, decreases in neuroticism, and increases in mindful awareness[33–35]. In terms of the neurobiological pattern, the psilocybin administration acutely resulted in increased global connectivity with reduced modularity[36–38]. Region-wise, there were reports of decreased activity in the thalamus, posterior cingulate cortex, medial prefrontal cortex[10], and altered connectivity of the claustrum[39]. Network-

wise, decreased connectivity was reported within the default mode network (DMN)[1,10], visual network[1], and executive control network (ECN)[40], as well as reduced segregation of the dorsal attentional network and ECN[41]. These neural counterparts indicate that the subjective effects of psilocybin are linked to alterations in the activity and connectivity of important brain regions involved in information integration and routing when averaged signal analysis is concerned. Dynamic analyses of connectivity patterns after psilocybin administration have shown that the brain tended to recurrently configure into transient functional patterns with low stability[42]. In addition, under psilocybin, there were higher probabilities for the brain to configure into a connectivity pattern characterized by a global cortex-wide positive phase coherence[43]. In terms of state transition dynamics, a recent study calculated the minimum network control energy required to transition between states (or maintain the same state) and found that the network control energy landscape was flattened under LSD and psilocybin, meaning that there were more frequent state transitions and increased entropy of brain pattern dynamics[44]. Taken together, averaged and dynamic connectivity analyses suggest that psilocybin alters brain function, such that the overall neurobiological pattern becomes functionally more connected, more fluid, and less modular.

Of interest is the link between the psychedelic state's neurobiological and phenomenological patterns as they are often analyzed separately. A recent investigation tried to correlate the occurrence rates of prominent connectivity patterns (i.e., frontoparietal subsystem and a globally coherent pattern) with subjective drug intensity (SDI) measured on a 10-point Likert scale[43,45]. As much as this approach has provided insights into the ensuing psychedelic state, it can be argued that, due to its simplicity, the SDI cannot capture the complexity of the psychedelic state's phenomenological pattern. Here, we adopt a neurophenomenological approach after psilocybin intake to quantify its effects on cerebral functional dynamics and link these dynamic spatiotemporal fingerprints with reported experiential alterations measured with psychometric instruments.

Results

Data was collected from 49 healthy participants who had previous experience with a psychedelic drug but not within the past three months[1]. Participants were allocated to two groups after being randomized to receive a single dose of psilocybin (0.17 mg/kg, n=22 (12 male, age=23±2.9 y) or placebo (bittering agent; n=27 (15 male, age=23.1±3.8 y). Six minutes of resting state with eyes open were acquired on a fMRI ultra-high field 7T scanner during the peak subjective drug effect (102 min post-treatment). The 5-Dimensional Altered States of Consciousness (5D-ASC) Rating Scale [26,46] was retrospectively evaluated at 360 min after drug administration.

Psilocybin administration leads to a distinct phenomenological pattern. The psychedelic state's phenomenological pattern was assessed using the 5D-ASC and its 11-ASC factors (see Methods) and were first assessed for normality assumptions. Shapiro-Wilk tests set at α=0.05 showed that all variables violated the assumption of normality (Table S1). As a result, Mann-Whitney U tests were used to compare the phenomenological outcomes in the two groups. Analyses revealed significant differences in all dimensions and factors with large effect sizes, such that the psilocybin group had more substantial effects than the placebo (Figure 1A and 1B, Table 1).

Functional connectivity and BOLD signal amplitude change after psilocybin administration. To investigate the neural effects of psilocybin, we first estimated the average functional connectome of each subject over the acquisition time. We used the Schaefer atlas to parcellate the brain into 100 distinct regions of interest (ROI) and computed Pearson correlations between pairs of ROIs. We found that after administration of psilocybin, whole-brain averaged connectivity increased (independent t-test: t=3.087, p=0.004; Figure 2A). This overall increase was further observed as a cortex-wide increase in the connectivity matrix values (independent t-test on the between-region connectivity values with FDR correction; Figure 2B). These alterations in the connectivity values were also accompanied by changes in the BOLD signal amplitude. By calculating the Euclidean norm of the BOLD time series related to each ROI, we found that regional BOLD signal amplitude

decreased after psilocybin administration in both posterior and anterior regions compared to the placebo group (independent t-test, FDR-corrected; Figure 2C, and Figure S1). While somatomotor, limbic network and temporal regions of the DMN did not show significant changes in their signal norm, the highest decrease in BOLD signal amplitude was related to the posterior cingulate cortex and parietal regions of the ECN.

Next, we investigated the effect of psilocybin administration on dynamic changes of the whole-brain functional connectome by estimating phase-based coherence connectivity matrices at each time point of the ROI time series. After concatenating all connectivity matrices across participants, we applied K-means clustering to summarize them into four connectivity patterns (Figure 2D). Variant and distinct patterns of complex inter-areal interactions emerged: one of both correlations and anti-correlations (Pattern 1), one of anti-correlations of the DMN with other networks (Pattern 2), one of global cortex-wide positive connectivity (Pattern 3), and one of low inter-areal connectivity (Pattern 4). Pattern 3 occurred significantly more often in the psilocybin group when compared to the placebo group (independent t-test: t=3.731, p=0.001, $\alpha_{\mathrm{bonferroni}} = 0.05/4 = 0.0125$, Figure 2D). Furthermore, using Markov modeling and considering each of the four patterns as model states, we estimated the transition probabilities of each state to the others. The psilocybin group showed significantly higher transition probabilities towards Pattern 3 from Pattern 1 (Wilcoxon Rank-Sum test: z=2.744, p=0.006), Pattern 3 (z=2.291, p=0.022), and Pattern 4 (z=2.000, p=0.045; Figure 2E). In addition, the psilocybin group showed lower transition probabilities from Pattern 2 to itself compared to the placebo group (z=-2.452, p=0.014).

The recurrent pattern of global hyperconnectivity is primarily associated with experiences of oceanic boundlessness and secondly with visionary restructuralization. To investigate the neurophenomenological counterpart of psilocybin intake, canonical correlation analysis (CCA) was performed between the 11-ASC factors and the pattern transition probabilities. CCA is a method of assessing the relationship between two multivariate datasets by maximizing their shared correlation

while reducing the potential of type-I error[47]. For this purpose, we estimated the first canonical vector for both the behavioral and neural space that maximizes the shared correlation between two spaces ($r=0.97$, $p<0.001$). Considering the neural space, the transition probabilities from Pattern 1 to Pattern 3 showed the highest correlation with the first canonical vector of the neural space ($r=0.86$, $p<0.001$, Figure 3A). Transitions from Pattern 2 to Pattern 1 ($r=0.47$, $p=0.015$) and from Pattern 4 to Pattern 3 ($r=0.40$, $p=0.048$) showed lower significant correlations with the first canonical vector of the neural space. At the same time, in the phenomenological space, factors related to oceanic boundlessness (experience of unity: $r=0.80$, $p<0.001$, blissful state: $r=0.74$, $p<0.001$, insightfulness: $r=0.68$, $p<0.001$, spiritual experience: $r=0.62$, $p<0.001$, and disembodiment: $r=0.35$, $p=0.036$) and visionary restructuralization (elementary imagery: $r=0.67$, $p<0.001$, audio-video synesthesia: $r=0.61$, $p<0.001$, complex imagery: $r=0.50$, $p=0.001$, and changed meaning of percept: $r=0.50$, $p=0.001$) showed the highest correlations with the first canonical vector of the phenomenological space (Figure 3B). To validate the results, we performed another CCA analysis between the dimensions of the 5D-ASC and the between-state transition probabilities. At the neural space, the transition probability from Pattern 1 to Pattern 3 showed the highest correlation with the first canonical vector of the neural space ($r=0.89$, $p<0.001$), and at the phenomenological space, oceanic boundlessness showed the highest correlation with the first canonical vector of the phenomenological space ($r=0.93$, $p<0.001$; Table 2). These observations show that the experiences of oceanic boundlessness and visual restructuralization after psilocybin administration are primarily associated with the cerebral functional tendency to reconfigure into a global cortex-wide positive connectivity pattern.

Discussion

We investigated the effect of the serotonergic hallucinogen psilocybin on the brain's functional connectome to link them with alternations of conscious experience to better comprehend how the resulting neural and experiential changes are interconnected. Overall, we found that psilocybin

158 administration led to a tendency of the brain to recurrently configure in a globally hyperconnected
159 pattern, which was linked to heightened reports of oceanic boundlessness (experience of unity,
160 blissfulness, insightfulness, and spiritual experience), and visionary restructuralization (complex
161 imagery, elementary imagery, audio-visual synesthesia, and changed meaning of percepts).

162 In terms of phenomenological changes, we report significant increases in all phenomenological
163 dimensions and factors in the psilocybin group over the placebo. This includes increased reports of
164 derealization, depersonalization, loss of self-control phenomena, elementary and complex visual
165 pseudo-hallucinations, audio-visual synesthesia, experiences of unity, spiritual experience, bliss,
166 insightfulness, and disembodiment[46], as we previously reported[1]. These findings evidence that a
167 moderate dose of psilocybin is enough to produce a significantly distinct phenomenological pattern
168 when compared to a placebo. Previous research on psilocybin administration also found that dosages
169 ranging from 45 to 315 μg/kg body weight produced measurable changes in oceanic boundlessness
170 (OBN), visionary restructuralization (VRS), auditory alternations (AUA), vigilance reduction
171 (VIR), and general altered states score (G-ASC) compared to placebo[48]. Additional research found
172 that 260 μg/kg body weight of psilocybin produced significant changes in OBN, dread of ego
173 dissolution (DED), and VRS when compared to placebo, ketanserin, and psilocybin with a
174 pretreatment of ketanserin conditions[49]. Taken together, our data replicates the general, dose-
175 dependent, phenomenological pattern associated with psilocybin consumption.

176 In terms of neural changes, we observed an overall increase in whole-brain functional
177 connectivity in the psilocybin group, in line with previous reports[37,38]. Previous work showed that
178 serotonergic psychedelics, including psilocybin, changed the brain's functional organization into a
179 new architecture, characterized by greater global integration, namely a higher amount of short-range
180 and long-range functional connections[42,50]. This dynamic analysis evidenced that, under psilocybin,
181 the brain had a higher probability of transitioning to a hyperconnected pattern compared to the
182 placebo group. Similar configurations and dynamic transitions have been reported by other studies

183 with psychedelic drugs, as well[43]. This hyperconnected pattern is characterized by maximal
184 integration and minimal segregation[51] and is interpreted as being functionally non-specific[43]. The
185 significantly higher occurrence rate of this hyperconnected pattern in the psychedelic state can be
186 explained by the "flattened landscape" theory[52]. Based on this dynamic systems approach, specific
187 connectivity patterns, which act as attractors in typical conditions, become less dominant under
188 psychedelics. Consequently, the brain expends less energy transitioning between these states[44]. This
189 supports that the occurrence rate of functionally specific patterns in our analysis results in increased
190 transition probabilities to enter the functionally non-specific hyperconnected pattern.

191 Moreover, we observed that this hyperconnectivity pattern is accompanied by cortex-wide
192 decreases in the BOLD signal amplitude in the psilocybin group. We here decided to retain the
193 global signal (GS) in the analysis pipeline, while acknowledging the significant debate around its
194 removal as part of the denoising process[53]. On one hand, the GS has demonstrated a neuronal
195 counterpart[54,55]., on the other, it was shown to reflect fMRI nuisance sources such as motion, scanner
196 artifacts, respiration[56], cardiac rate[57], and vascular activity[58,59]. Our choice to keep the GS is justified
197 by our recent finding that it can act as a complementary metric to extracted connectivity patterns[60].
198 Specifically, we found that when the hyperconnected pattern was accompanied by high GS
199 amplitude during wakeful rest, it was more probable for participants to report phenomenological
200 instances of mind blanking[60] (i.e., the subjective evaluation of having no thoughts during
201 unconstrained mentation[61]). The amplitude of the GS has been previously shown to act as an indirect
202 measure of general arousal levels. For example, higher GS amplitude was related to lower levels of
203 arousal, and lower GS amplitudes were linked to higher levels of arousal[62–65]. Indeed, it was
204 demonstrated that the GS amplitude correlated positively with the relative amplitude of the delta
205 band of EEG oscillations and negatively with the relative amplitude of the alpha band[64]. In the
206 current study, we show that the hyperconnectivity pattern is accompanied by reduced GS amplitude,
207 therefore adding to the explanation of the psychedelic state as mediated by high cortical arousal[66].

In terms of neurophenomenology, we show that higher transition probabilities into the hyperconnected pattern are significantly associated with the factors of oceanic boundlessness (OBN) and visionary restructuralization (VRS). OBN is characterized by deeply felt positive mood, feelings of insight, and experiences of unity[26]. Previous studies associated positively experienced ego dissolution and oceanic boundlessness with reduced levels of hippocampal glutamate[1] and higher feelings of insight with reduced levels of DMN within-network static functional connectivity[28]. Our whole-brain dynamic analysis complements this literature by showing that the brain's tendency to be recurrently hyperconnected after psilocybin intake can also explain the experiences of unity. This is important as this factor is characterized by a disruption of the self-world boundary[1] and the hyperconnected pattern is characterized by an atypical minimal segregation profile[51]. Other studies showed that both integration and segregation are necessary for a coherent sense of self[67]. Given these two main findings, we postulate that the reported feelings of unity and visual pseudo-hallucinatory experiences under psilocybin are connected to the brain's inclination to exhibit highly integrated patterns, thereby evidencing the brain's capacity to entertain diverse mental associations. This can be supported by the fact that different dimensions of creative thinking improve after psilocybin intake as a result of increased between-network functional connectivity of DMN and frontoparietal network,[28] a connectivity profile also seen in the hyperconnected pattern.

Interestingly, three of the five factors of OBN (unity, bliss, insight) represented the highest canonical correlations in our analysis, while the visual restructuralization (VRS) factors followed. This was further supported by canonical correlations performed at the dimensional level, which showed OBN as having the highest association with transition probabilities to the hyperconnected pattern comparatively. This is a unique finding given that serotonergic psychedelics are sometimes referred to as hallucinogens, leaving one to assume that their primary effects are hallucinatory in nature[4]. Indeed, such an issue can be seen historically in the etymology of these drugs as they have been referred to as psychotomimetics, psycholytics, hallucinogens, psychedelics, or entheogens at

233 different points in time[4,68]. Psilocybin-assisted therapy studies also show that the clinical outcome
234 is driven primarily by OBN, supporting its primary role in the drug's phenomenological effect[69].
235 OBN's central importance is further supported by its association with decreased 5-HT2AR binding
236 potential in cortical regions,[48,49] its ability to predict medial prefrontal cortex-posterior cingulate
237 cortex functional connectivity changes,[70] and its positive correlation with disconnection of
238 somatomotor network correlates[71]. Since OBN is defined as the positive valence associated with
239 depersonalization and derealization through factors such as unity, that require dissolution of the self-
240 world boundary, it can be seen primarily as a psychometric dimension that describes
241 phenomenological modifications of the ego[26,46]. Our data, along with previous research, suggests
242 that OBN is the primary driver of the psychedelic state's general phenomenological pattern. As a
243 consequence, future work might provide more refined terminologies to capture this driving effect
244 of psilocybin, such as "egotropic" over "hallucinogenic".

245 Our study is subject to various limitations. First, at the group level, the administration of
246 psilocybin was not high enough to induce total ego dissolution for all participants. The administered
247 dose was selected to be sufficient to induce a psychedelic state that participants could endure in an
248 ultra-high field scanner environment. However, our phenomenological analysis showed that this
249 dosage was adequate. Second, the lack of concurrent physiological recordings during fMRI scanning
250 limits proper tracking of arousal levels. In this study, we used the GS amplitude as a proxy for the
251 level of cortical arousal. At the same time, the absence of simultaneous electrophysiological
252 recordings limits the direct interpretation of neuronal firing during hyperconnected patterns.
253 Simultaneous physiological and electrophysiological recordings in future studies can help to better
254 investigate the role of cortical and general arousal with neuronal firing patterns in producing
255 mystical experiences during the psychedelic state. Finally, the data-driven nature of the analysis can
256 limit the results of the current study to the recruited population. However, this is less concerning in
257 the dynamic functional connectivity analysis as in our previous studies it was shown that similar

258 recurrent connectivity patterns can be derived in different datasets and different brain parcellations,
259 showing their replicability and universality[51,60].

260 In conclusion, we found that pharmacological perturbations using psilocybin generate profound
261 alterations both at the brain and at the experiential level. We showed that administration of
262 psilocybin leads to an increase in the brain's tendency to configure into a functionally non-specific
263 hyperconnected organization, which phenomenologically associates with experiences of oceanic
264 boundlessness and visual pseudo-hallucinations. The present findings illuminate the intricate
265 interplay between brain dynamics and subjective experience under psilocybin, providing new
266 insights into the neurophenomenology and neurophysiology of the psychedelic state.

267 **Methods**

268 **Participants.** Data were collected from 49 healthy participants with previous experience with a
269 psychedelic drug, but not within the past 3 months of the experiment. Participants were randomized
270 to receive a single dose of psilocybin (0.17 mg/kg, n=22; 12 male; age=23±2.9 y) or placebo (n=27;
271 15 male; age=23.1±3.8 y). This study was conducted according to the code of ethics on human
272 experimentation established by the Declaration of Helsinki (1964) and amended in Fortaleza (Brazil,
273 October 2013). This study is in accordance with the Medical Research Involving Human Subjects
274 Act (WMO) and was approved by the Academic Hospital and the University's Medical Ethics
275 Committee (Maastricht University, Netherlands Trial Register: NTR6505). All participants were
276 fully informed of all procedures, possible adverse reactions, legal rights, responsibilities, expected
277 benefits, and their right to voluntary termination without consequences.

278 **Datasets.** Six minutes of resting state fMRI were acquired from the participants with eyes open
279 during peak subjective drug effect (102 minutes post-treatment). In addition, the 5-Dimensional
280 Altered States of Consciousness (5D-ASC) Rating Scale was administered 360 minutes after drug
281 intake, as retrospective phenomenological assessments of the drug experience.

Phenomenological Assessment. The 5D-ASC Rating Scale is a 94-item self-report scale that assesses the participants' alterations from normal waking consciousness[46]. In this questionnaire, participants are asked to make a vertical mark on the 10-cm line below each statement to rate the extent to which the following statements applied to their experience: "No, not more than usual" to "Yes, more than usual." The 5D-ASC comprises five dimensions, including *oceanic boundlessness* (OBN), *dread of ego dissolution* (DED), *visionary restructuralization* (VRS), auditory *alterations* (AUA), and *vigilance reduction* (VIR). Further, OBN, DED, and VRS can be decomposed into 11 subscales via a previously published factor analysis[26]: OBN: *experience of unity*, *spiritual experience*, *blissful state*, *insightfulness*, *disembodiment*, DED: *impaired control and cognition*, *anxiety*, and VRS: *complex imagery*, *elementary imagery*, *audio-visual synesthesia*, and *changed meaning of percepts* comprising the 11-ASC scoring scheme.

Imaging Setup. Images were acquired on a 7T Siemens Magnetom scanner (Siemens Medical, Erlangen, Germany) using 32 receiving channel head array Nova coil (NOVA Medical Inc., Wilmington MA). The T1w images were acquired using a magnetization-prepared 2 rapid acquisition gradient-echo (MP2RAGE) sequence collecting 190 sagittal slices following parameters: repetition time (TR) = 4500 ms, echo time (TE) = 2.39 ms, inversion times TI1 /TI2 = 900/2750 ms, flip angle1 = 5°, flip angle2 = 3°, voxel size = 0.9 mm isotropic, bandwidth = 250 Hz/pixel. In addition, 258 whole-brain EPI volumes were acquired at rest (TR = 1400 ms; TE = 21 ms; field of view=198 mm; flip angle = 60°; oblique acquisition orientation; interleaved slice acquisition; 72 slices; slice thickness = 1.5 mm; voxel size = 1.5 × 1.5 × 1.5 mm).

Phenomenological Analysis. 5D-ASC and its 11-ASC factors were assessed for normality assumptions using Shapiro-Wilk tests set at α=0.05. Due to violations in normality, non-parametric Mann-Whitney U tests were performed to compare the 5D-ASC and 11-ASC scores between the two groups. P-values were corrected using the Bonferroni method with a significance level of set at α=0.05. The effect size was calculated based on Glass rank biserial coefficient (rg).

307 **Neuroimaging Data Preprocessing.** fMRI data were preprocessed using a locally developed
308 pipeline based on SPM12[72]. After susceptibility distortion correction and realignment, functional
309 data were registered to the high-resolution T1 image, then normalized to the standard MNI space,
310 and finally smoothed using a Gaussian kernel with a full width at half maximum (FWHM) of 6mm.
311 After segmentation of the structural T1 image into grey matter (GM), white matter (WM), and CSF
312 masks, the bias-corrected structural image and all the extracted masks were normalized to the MNI
313 space. Further, WM and CSF masks were eroded by one voxel to remove any overlapping between
314 these tissues and the GM voxels. To denoise functional time series, we used a locally developed
315 pipeline written in Python [nipype package[73]]. In this pipeline, a general linear model (GLM) was
316 fitted to each voxel data separately, regressing out the effect of six movement parameters
317 (translation in x, y, and z directions, and rotation in yaw, roll, and pitch directions) and their first
318 derivative, constant and linear trends using zero-order and first-order Legendre polynomials, 5
319 principal components of signals in the WM and CSF masks, and outlier data points. Outlier detection
320 was performed using the ART toolbox (http://web.mit.edu/swg/software.htm). Any volume with a
321 movement value of greater than 3 mm, rotation value of greater than 0.05 radians, and z-normalized
322 global signal intensity of greater than 3 was considered an outlier. After regressing out these
323 nuisance regressors, the remaining signal was filtered in the range of [0.008, 0.09] Hz and was used
324 for further analysis. The Schaefer atlas with 100 ROIs and a resolution of 2mm[74] was used to extract
325 the averaged BOLD signals inside each ROI.

326 **Averaged Functional Connectivity.** Pearson correlations were calculated between the BOLD
327 time series for every pair of ROIs, subsequently Fisher transformed, resulting in the generation of a
328 100×100 connectivity matrix for each individual participant. An Independent t-test was used to
329 compare the 4950 possible between-region connectivity values between the two groups. FDR
330 correction was performed to correct for multiple comparisons. Further, the average of the
331 connectivity values over the whole brain was calculated for each participant and was considered as

the overall connectivity value of the brain. An independent t-test was performed to compare the overall connectivity values between psilocybin and placebo groups.

Time-varying Functional Connectivity. We used phase-based coherence analysis to extract between-region connectivity patterns at each time point of the scanning session[51,75]. For each participant i, after z-normalization of time series at each region r (i.e., $x_{i,r}[t]$), the instantaneous phase of each time series was calculated via Hilbert transform as:

$$\hat{x}_{i,r}(t) = \frac{1}{\pi t} * x_{i,r}(t)$$

where * indicates a convolution operator. Using this transformation, we produced an analytical signal for each regional time series as:

$$x_{i,r}^{a}(t) = x_{i,r}(t) + j\hat{x}_{i,r}(t)$$

where $j = \sqrt{-1}$. From this analytical signal, the instantaneous phase of each time series can be estimated as:

$$\varphi_{i,r}(t) = \tan^{-1}\left(\frac{\hat{x}_{i,r}(t)}{x_{i,r}(t)}\right)$$

After wrapping each instantaneous phase signal of $\varphi_{i,r}(t)$ to the $[-\pi, \pi]$ interval and naming the obtained signal as $\theta_{i,r}(t)$, we calculated a connectivity measure for each pair of regions as the cosine of their phase difference. For example, the connectivity measure between regions r and s in subject i was defined as:

$$conn_{i,r,s}(t) \triangleq \cos\left(\theta_{i,r}(t) - \theta_{i,s}(t)\right)$$

By this definition, completely synchronized time series lead to a connectivity value of 1, completely desynchronized time series produce a connectivity value of zero, and anticorrelated time series produce a connectivity measure of -1. Using this approach, we created a connectivity matrix of 100×100 at each time point t for each subject i that we called $C_i(t)$:

$$C_i(t) \triangleq \left[conn_{i,r,s}(t)\right]_{r,s}$$

After collecting the connectivity matrices across all time points and participants, k-means clustering was applied, with 500 repetitions and 200 iterations at each repetition. With this technique, four robust and reproducible patterns were extracted as the centroids of the clusters, and each resting connectivity matrix was assigned to one of the extracted patterns.

We calculated the occurrence rate of each pattern defined as the proportion of connectivity matrices assigned to that pattern and was calculated for each subject separately. Independent two-tailed t-tests were used to compare the occurrence rate of each FC pattern between the psychedelic and placebo groups. Bonferroni correction was used to correct the p-values for multiple comparisons across the four connectivity patterns.

Dynamic state transition modeling. To investigate the temporal evolution of the identified connectivity matrices, we defined the extracted patterns as the distinct states of a dynamical system transitioning between them over time using Markov modelling[51]. Using this approach, the data of a sample participant could be stated as a sequence of connectivity patterns over time (i.e., $\{P_t \mid t: 1, \dots, T \; and \; P_t \in \{1, \dots, M\}\}$, where M is the number of patterns and T is the number of signal time points). In this case, the probability of transitioning from Pattern I to Pattern J defined as $p(I \rightarrow J)$, considering $I, J \in \{1, .., M\}$, can be calculated as the number of consecutive I, J pairs in the sequence, divided by the total number of transitions from pattern I:

$$p(I \rightarrow J) = \frac{\sum_{t=0}^{T-1}[(P_t == I) \,\&\, (P_{t+1} == J)]}{\sum_{j=1}^{M}\sum_{t=0}^{T-1}[(P_t == I) \,\&\, (P_{t+1} == j)]}$$

This transition probability was estimated for each possible between-state transition and each subject separately. With this approach, we could compare any significant difference in transition probabilities between two groups of subjects. To detect significantly different transition

probabilities between the two groups, Wilcoxon rank-sum test was performed on each transition and p-values were FDR-corrected.

Regional BOLD Amplitude Analysis. The Euclidean norm of the BOLD signal was calculated at each ROI as a measure of the power of the signal. Independent t-test was used to compare the regional GS power between two groups and p-values were FDR-corrected due to multiple comparisons.

Neurophenomenological Analysis. A canonical correlation (CCA) analysis was conducted using the sixteen dynamic patterns transition probability variables as features of the neuronal space, and the 11-ASC and EDI variables as features of the phenomenological space, to evaluate the multivariate shared relationship between the two variable sets. CCA is a multivariate latent variable model that identifies associations between two different data modalities[47]. Considering matrix $X^{N\times M}$ contains M neuronal features of N subjects, and $Y^{N\times P}$ contains P phenomenological features of N subjects, the objective of the CCA is to find pairs of neuronal and phenomenological weights $w_x^{M\times 1}$ and $w_y^{P\times 1}$ such that the weighted sum of the neuronal and phenomenological variables maximizes the correlation between the resulting latent variables (canonical variates):

$$\max_{w_x, w_y} corr(Xw_x, Yw_y)$$

After finding latent variables Xw_x and Yw_y that have the maximal correlation, the features in each modality of data that have a stronger correlation with their respective latent variable are also significantly associated with one another.

Data availability

The connectomes and the accompanying covariates used to differentiate individuals can be made available to qualified research institutions upon reasonable request to J.G.R. and a data use agreement executed with Maastricht University.

Code availability

All codes used for analysis are freely available at https://gitlab.uliege.be/S.Mortaheb/psychedelics

Author contributions

JR & AD contributed to the conception and design of the work; NM acquired the data; SM & LDF contributed with data analysis; all authors contributed to data interpretation; SM, LF, & AD drafted and revised the manuscript; all authors proofread the submitted work.

Acknowledgments

This article was supported by the Belgian Fund for Scientific Research (FRS-FNRS), the European Union's Horizon 2020 Research and Innovation Marie Skłodowska-Curie RISE program NeuronsXnets (grant agreement 101007926), the European Cooperation in Science and Technology COST Action (CA18106), the Léon Fredericq Foundation, and the University and of University Hospital of Liège.

412 **References**

413 1. Mason, N. L. *et al.* Me, myself, bye: regional alterations in glutamate and the experience of ego
414 dissolution with psilocybin. *Neuropsychopharmacol.* **45**, 2003–2011 (2020).
415 2. Metzner, R. Hallucinogenic Drugs and Plants in Psychotherapy and Shamanism. *Journal of*
416 *Psychoactive Drugs* **30**, 333–341 (1998).
417 3. Volgin, A. D. *et al.* Understanding Central Nervous System Effects of Deliriant Hallucinogenic Drugs
418 through Experimental Animal Models. *ACS Chem. Neurosci.* **10**, 143–154 (2019).
419 4. Nichols, D. E. Psychedelics. *Pharmacol Rev* **68**, 264–355 (2016).
420 5. Kwan, A. C., Olson, D. E., Preller, K. H. & Roth, B. L. The neural basis of psychedelic action. *Nat*
421 *Neurosci* **25**, 1407–1419 (2022).
422 6. Moreno, et al. Safety, Tolerability, and Efficacy of Psilocybin in 9 Patients With Obsessive-
423 Compulsive Disorder. (2006).
424 7. Grob, C. S. *et al.* Pilot Study of Psilocybin Treatment for Anxiety in Patients With Advanced-Stage
425 Cancer. *Arch Gen Psychiatry* **68**, 71 (2011).
426 8. Andersen, K. A. A., Carhart-Harris, R., Nutt, D. J. & Erritzoe, D. Therapeutic effects of classic
427 serotonergic psychedelics: A systematic review of modern-era clinical studies. *Acta Psychiatr. Scand.*
428 **143**, 101–118 (2021).
429 9. Carhart-Harris, R. L. *et al.* Trial of Psilocybin versus Escitalopram for Depression. *N Engl J Med* **384**,
430 1402–1411 (2021).
431 10. Carhart-Harris, R. L. *et al.* Neural correlates of the psychedelic state as determined by fMRI studies
432 with psilocybin. *Proc. Natl. Acad. Sci. U.S.A.* **109**, 2138–2143 (2012).
433 11. Ross, S. *et al.* Rapid and sustained symptom reduction following psilocybin treatment for anxiety and
434 depression in patients with life-threatening cancer: a randomized controlled trial. *J Psychopharmacol*
435 **30**, 1165–1180 (2016).
436 12. Carhart-Harris, R. L. *et al.* Psilocybin with psychological support for treatment-resistant depression: an
437 open-label feasibility study. *The Lancet Psychiatry* **3**, 619–627 (2016).

13. Carhart-Harris, R. L. *et al.* Psilocybin for treatment-resistant depression: fMRI-measured brain mechanisms. *Sci Rep* **7**, 13187 (2017).
14. Carhart-Harris, R. L. *et al.* Psilocybin with psychological support for treatment-resistant depression: six-month follow-up. *Psychopharmacology* **235**, 399–408 (2018).
15. Davis, A. K. *et al.* Effects of Psilocybin-Assisted Therapy on Major Depressive Disorder: A Randomized Clinical Trial. *JAMA Psychiatry* **78**, 481 (2021).
16. Griffiths, R. R. *et al.* Psilocybin produces substantial and sustained decreases in depression and anxiety in patients with life-threatening cancer: A randomized double-blind trial. *J Psychopharmacol* **30**, 1181–1197 (2016).
17. Anderson, B. T. *et al.* Psilocybin-assisted group therapy for demoralized older long-term AIDS survivor men: An open-label safety and feasibility pilot study. *EClinicalMedicine* **27**, 100538 (2020).
18. Johnson, M. W., Garcia-Romeu, A. & Griffiths, R. R. Long-term follow-up of psilocybin-facilitated smoking cessation. *The American Journal of Drug and Alcohol Abuse* **43**, 55–60 (2017).
19. Bogenschutz, M. P. *et al.* Psilocybin-assisted treatment for alcohol dependence: A proof-of-concept study. *J Psychopharmacol* **29**, 289–299 (2015).
20. Garcia-Romeu, A. *et al.* Cessation and reduction in alcohol consumption and misuse after psychedelic use. *J Psychopharmacol* **33**, 1088–1101 (2019).
21. Johnson, M. W., Garcia-Romeu, A., Cosimano, M. P. & Griffiths, R. R. Pilot study of the 5-HT $_{2A}$ R agonist psilocybin in the treatment of tobacco addiction. *J Psychopharmacol* **28**, 983–992 (2014).
22. Bayne, T. & Carter, O. Dimensions of consciousness and the psychedelic state. *Neuroscience of Consciousness* **2018**, niy008 (2018).
23. Greene, A. S., Horien, C., Barson, D., Scheinost, D. & Constable, R. T. Why is everyone talking about brain state? *Trends Neurosci* **46**, 508–524 (2023).
24. Rock, A. J. & Krippner, S. Does the Concept of "Altered States of Consciousness" Rest on a Mistake? *IJTS* **26**, 33–40 (2007).
25. Nour, M. M. & Carhart-Harris, R. L. Psychedelics and the science of self-experience. *Br J Psychiatry* **210**, 177–179 (2017).

26. Studerus, E., Gamma, A. & Vollenweider, F. X. Psychometric Evaluation of the Altered States of Consciousness Rating Scale (OAV). *PLoS ONE* **5**, e12412 (2010).

27. Girn, M., Mills, C., Roseman, L., Carhart-Harris, R. L. & Christoff, K. Updating the dynamic framework of thought: Creativity and psychedelics. *NeuroImage* **213**, 116726 (2020).

28. Mason, N. L. *et al.* Spontaneous and deliberate creative cognition during and after psilocybin exposure. *Transl Psychiatry* **11**, 209 (2021).

29. Carhart-Harris, R. L. *et al.* The entropic brain: a theory of conscious states informed by neuroimaging research with psychedelic drugs. *Front. Hum. Neurosci.* **8**, (2014).

30. Griffiths, R. R., Richards, W. A., McCann, U. & Jesse, R. Psilocybin can occasion mystical-type experiences having substantial and sustained personal meaning and spiritual significance. *Psychopharmacology* **187**, 268–283 (2006).

31. Preller, K. H. & Vollenweider, F. X. Phenomenology, structure, and dynamic of psychedelic states. *Behavioral neurobiology of psychedelic drugs* 221–256 (2018).

32. Majić, T., Schmidt, T. T. & Gallinat, J. Peak experiences and the afterglow phenomenon: When and how do therapeutic effects of hallucinogens depend on psychedelic experiences? *J Psychopharmacol* **29**, 241–253 (2015).

33. Erritzoe, D. *et al.* Effects of psilocybin therapy on personality structure. *Acta Psychiatr Scand* **138**, 368–378 (2018).

34. MacLean, K. A., Johnson, M. W. & Griffiths, R. R. Mystical experiences occasioned by the hallucinogen psilocybin lead to increases in the personality domain of openness. *J Psychopharmacol* **25**, 1453–1461 (2011).

35. Madsen, M. K. *et al.* A single psilocybin dose is associated with long-term increased mindfulness, preceded by a proportional change in neocortical 5-HT2A receptor binding. *European Neuropsychopharmacology* **33**, 71–80 (2020).

36. Daws, R. E. *et al.* Increased global integration in the brain after psilocybin therapy for depression. *Nat Med* **28**, 844–851 (2022).

37. Preller, K. H. *et al.* Psilocybin Induces Time-Dependent Changes in Global Functional Connectivity. *Biological Psychiatry* **88**, 197–207 (2020).

38. Roseman, L., Leech, R., Feilding, A., Nutt, D. J. & Carhart-Harris, R. L. The effects of psilocybin and MDMA on between-network resting state functional connectivity in healthy volunteers. *Front. Hum. Neurosci.* **8**, (2014).
39. Barrett, F. S., Krimmel, S. R., Griffiths, R. R., Seminowicz, D. A. & Mathur, B. N. Psilocybin acutely alters the functional connectivity of the claustrum with brain networks that support perception, memory, and attention. *NeuroImage* **218**, 116980 (2020).
40. McCulloch, D. E.-W., Madsen, M. K. & Stenb, D. S. Lasting effects of a single psilocybin dose on resting-state functional connectivity in healthy individuals. *Journal of Psychopharmacology* 11 (2022).
41. Madsen, M. K. *et al.* Psilocybin-induced changes in brain network integrity and segregation correlate with plasma psilocin level and psychedelic experience. *European Neuropsychopharmacology* **50**, 121–132 (2021).
42. Petri, G. *et al.* Homological scaffolds of brain functional networks. *J. R. Soc. Interface.* **11**, 20140873 (2014).
43. Lord, L.-D. *et al.* Dynamical exploration of the repertoire of brain networks at rest is modulated by psilocybin. *NeuroImage* **199**, 127–142 (2019).
44. Singleton, S. P. *et al.* Receptor-informed network control theory links LSD and psilocybin to a flattening of the brain's control energy landscape. *Nat Commun* **13**, 5812 (2022).
45. Olsen, A. S. *et al.* Psilocybin modulation of time-varying functional connectivity is associated with plasma psilocin and subjective effects. *NeuroImage* **264**, 119716 (2022).
46. Dittrich, A. The standardized psychometric assessment of altered states of consciousness (ASCs) in humans. *Pharmacopsychiatry* **31**, 80–84 (1998).
47. Mihalik, A. *et al.* Canonical Correlation Analysis and Partial Least Squares for Identifying Brain–Behavior Associations: A Tutorial and a Comparative Study. *Biological Psychiatry: Cognitive Neuroscience and Neuroimaging* **7**, 1055–1067 (2022).
48. Hasler, F., Grimberg, U., Benz, M. A., Huber, T. & Vollenweider, F. X. Acute psychological and physiological effects of psilocybin in healthy humans: a double-blind, placebo-controlled dose?effect study. *Psychopharmacology* **172**, 145–156 (2004).

49. Quednow, B. B., Kometer, M., Geyer, M. A. & Vollenweider, F. X. Psilocybin-Induced Deficits in Automatic and Controlled Inhibition are Attenuated by Ketanserin in Healthy Human Volunteers. *Neuropsychopharmacol* **37**, 630–640 (2012).
50. Tagliazucchi, E. *et al.* Increased Global Functional Connectivity Correlates with LSD-Induced Ego Dissolution. *Current Biology* **26**, 1043–1050 (2016).
51. Demertzi, A. *et al.* Human consciousness is supported by dynamic complex patterns of brain signal coordination. *Science Advances* **5**, eaat7603 (2019).
52. Carhart-Harris, R. L. & Friston, K. J. REBUS and the Anarchic Brain: Toward a Unified Model of the Brain Action of Psychedelics. *Pharmacol Rev* **71**, 316–344 (2019).
53. Murphy, K. & Fox, M. D. Towards a consensus regarding global signal regression for resting state functional connectivity MRI. *NeuroImage* **154**, 169–173 (2017).
54. Schölvinck, M. L., Maier, A., Ye, F. Q., Duyn, J. H. & Leopold, D. A. Neural basis of global resting-state fMRI activity. *Proc. Natl. Acad. Sci. U.S.A.* **107**, 10238–10243 (2010).
55. Xu, H. *et al.* Impact of global signal regression on characterizing dynamic functional connectivity and brain states. *NeuroImage* **173**, 127–145 (2018).
56. Power, J. D., Plitt, M., Laumann, T. O. & Martin, A. Sources and implications of whole-brain fMRI signals in humans. *NeuroImage* **146**, 609–625 (2017).
57. Chang, C. & Glover, G. H. Time–frequency dynamics of resting-state brain connectivity measured with fMRI. *NeuroImage* **50**, 81–98 (2010).
58. Zhu, D. C., Tarumi, T., Khan, M. A. & Zhang, R. Vascular Coupling in Resting-State FMRI: Evidence from Multiple Modalities. *J Cereb Blood Flow Metab* **35**, 1910–1920 (2015).
59. Colenbier, N. *et al.* Disambiguating the role of blood flow and global signal with partial information decomposition. *NeuroImage* **213**, 116699 (2020).
60. Mortaheb, S. *et al.* Mind blanking is a distinct mental state linked to a recurrent brain profile of globally positive connectivity during ongoing mentation. *Proceedings of the National Academy of Sciences* **119**, e2200511119 (2022).
61. Ward, A. F. & Wegner, D. M. Mind-blanking: when the mind goes away. *Front. Psychol.* **4**, (2013).

62. Fukunaga, M. *et al.* Large-amplitude, spatially correlated fluctuations in BOLD fMRI signals during extended rest and early sleep stages. *Magnetic Resonance Imaging* **24**, 979–992 (2006).

63. Nilsonne, G. *et al.* Intrinsic brain connectivity after partial sleep deprivation in young and older adults: results from the Stockholm Sleepy Brain study. *Sci Rep* **7**, 9422 (2017).

64. Wong, C. W., Olafsson, V., Tal, O. & Liu, T. T. The amplitude of the resting-state fMRI global signal is related to EEG vigilance measures. *NeuroImage* **83**, 983–990 (2013).

65. Liu, X. *et al.* Subcortical evidence for a contribution of arousal to fMRI studies of brain activity. *Nat Commun* **9**, 395 (2018).

66. Carhart-Harris, R. L. *et al.* Functional Connectivity Measures After Psilocybin Inform a Novel Hypothesis of Early Psychosis. *Schizophrenia Bulletin* **39**, 1343–1351 (2013).

67. Di Plinio, S., Perrucci, M. G., Aleman, A. & Ebisch, S. J. H. I am Me: Brain systems integrate and segregate to establish a multidimensional sense of self. *NeuroImage* **205**, 116284 (2020).

68. Metzner, R. Psychedelic, Psychoactive, and Addictive Drugs and States of Consciousness. in *Mind-altering drugs : the science of subjective experience* (Oxford ; New York : Oxford University Press, 2005).

69. Rotz, R. von *et al.* Single-dose psilocybin-assisted therapy in major depressive disorder: a placebo-controlled, double-blind, randomised clinical trial. *eClinicalMedicine* **56**, (2023).

70. Smigielski, L., Scheidegger, M., Kometer, M. & Vollenweider, F. X. Psilocybin-assisted mindfulness training modulates self-consciousness and brain default mode network connectivity with lasting effects. *NeuroImage* **196**, 207–215 (2019).

71. Preller, K. H. *et al.* Changes in global and thalamic brain connectivity in LSD-induced altered states of consciousness are attributable to the 5-HT2A receptor. *eLife* **7**, e35082 (2018).

72. Penny, W. D., Friston, K. J., Ashburner, J. T., Kiebel, S. J. & Nichols, T. E. *Statistical Parametric Mapping: The Analysis of Functional Brain Images*. (Elsevier, 2011).

73. Gorgolewski, K. *et al.* Nipype: A Flexible, Lightweight and Extensible Neuroimaging Data Processing Framework in Python. *Front. Neuroinform.* **5**, (2011).

74. Schaefer, A. *et al.* Local-Global Parcellation of the Human Cerebral Cortex from Intrinsic Functional Connectivity MRI. *Cerebral Cortex* **28**, 3095–3114 (2018).

575 75. Barttfeld, P. *et al.* Signature of consciousness in the dynamics of resting-state brain activity. *Proc.*
576 *Natl. Acad. Sci. U.S.A.* **112**, 887–892 (2015).
577

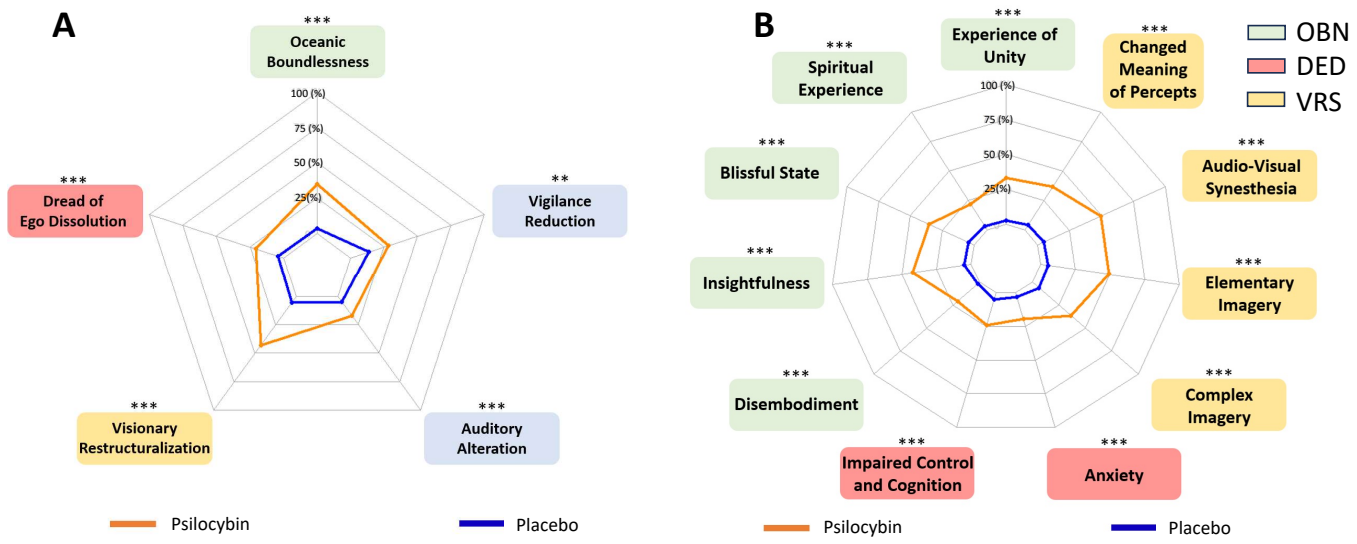

Figure 1. Substantial alterations in subjective experience were reported after psilocybin administration compared to placebo. A) The assessment of five dimensions of altered states of consciousness questionnaire (5D-ASC) showed that the administration of psilocybin significantly altered subjective experience in all dimensions. **B)** The same effect can also be observed considering the 11 factors of altered states of consciousness (11-ASC). Notes, OBN: Oceanic Boundlessness, DED: Dread of Ego Dissolution, VRS: Visionary Restructuralization. Radar plots illustrate group means for each dimension/factor.

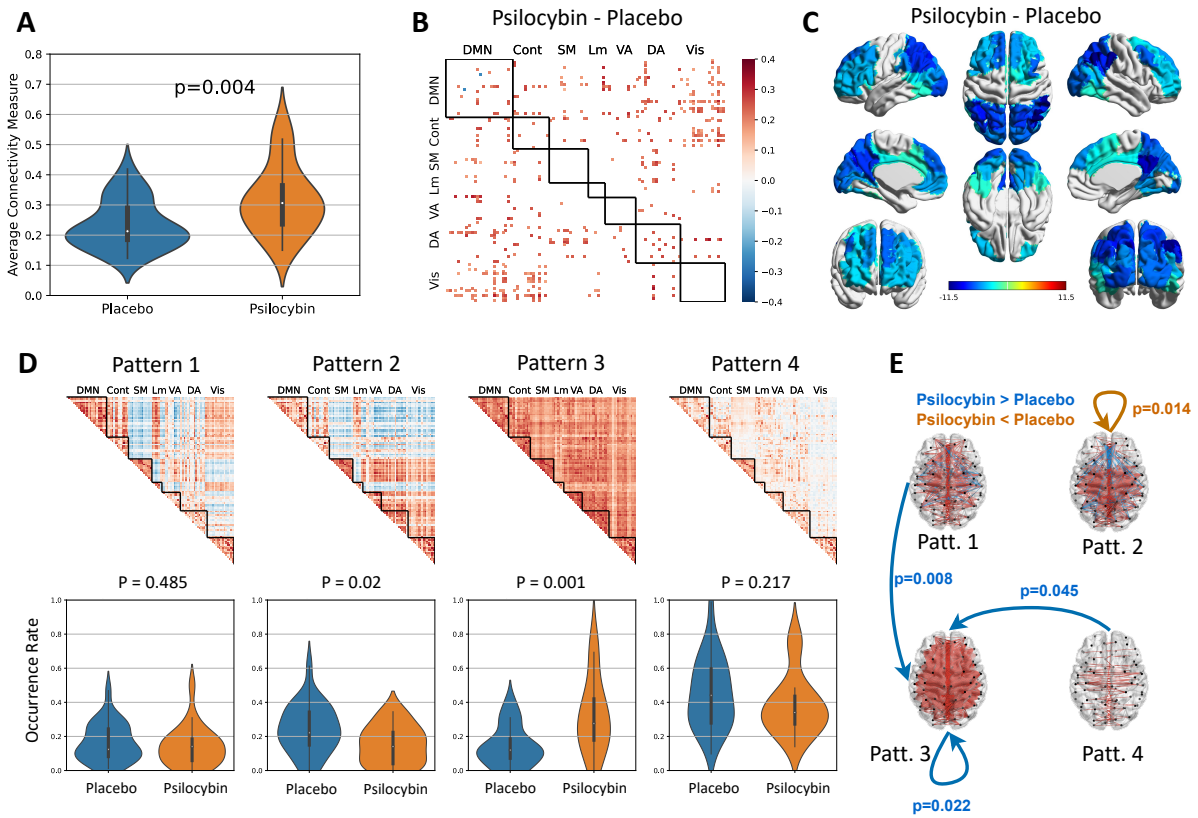

Figure 2. After psilocybin administration, there was an overall cerebral tendency to show more re-occurrence of a functional hyper-connectivity pattern. A) Averaged functional connectivity expressed as Fisher-transformed correlation values increased significantly after psilocybin administration compared to the placebo group. **B)** There were higher inter-regional connectivity values in the psilocybin group. The matrix represents the difference between the averaged connectivity matrix of the psilocybin group and that of the placebo group (contrast: psilocybin minus placebo). Only significant difference values are colored. **C)** The BOLD amplitude of posterior and anterior brain regions decreased after psilocybin administration, while the amplitude of somatomotor and limbic areas as well as the temporal regions of default more network remain unchanged. Colors are based on the difference values between the mean value of Euclidean norm of BOLD time series in the psilocybin group and the placebo group at each ROI; only significant difference values are colored. **D)** The functional connectome reconfigures in four connectivity patterns, ranging from complex inter-areal interactions (Pattern 1) to a low inter-areal

connectivity profile (Pattern 4). After psilocybin administration, there was a significant increase in the occurrence rate of the global cortex-wide positive connectivity (Pattern 3). The connectivity matrices are colored based on the connectivity value: from dark blue to dark red corresponds to connectivity values from -1 to +1. Violin plots represent the distribution of patterns' occurrence rates across participants. **E)** The transition probability from other patterns to Pattern 3 increased in the psilocybin group. Arrows indicate transitions between functional connectivity states. Blue corresponds to significantly higher transition probabilities (Wilcoxon Rank-Sum test) for the psilocybin group compared to the placebo, and orange corresponds to significantly higher transition probabilities for the placebo compared to the psilocybin group.

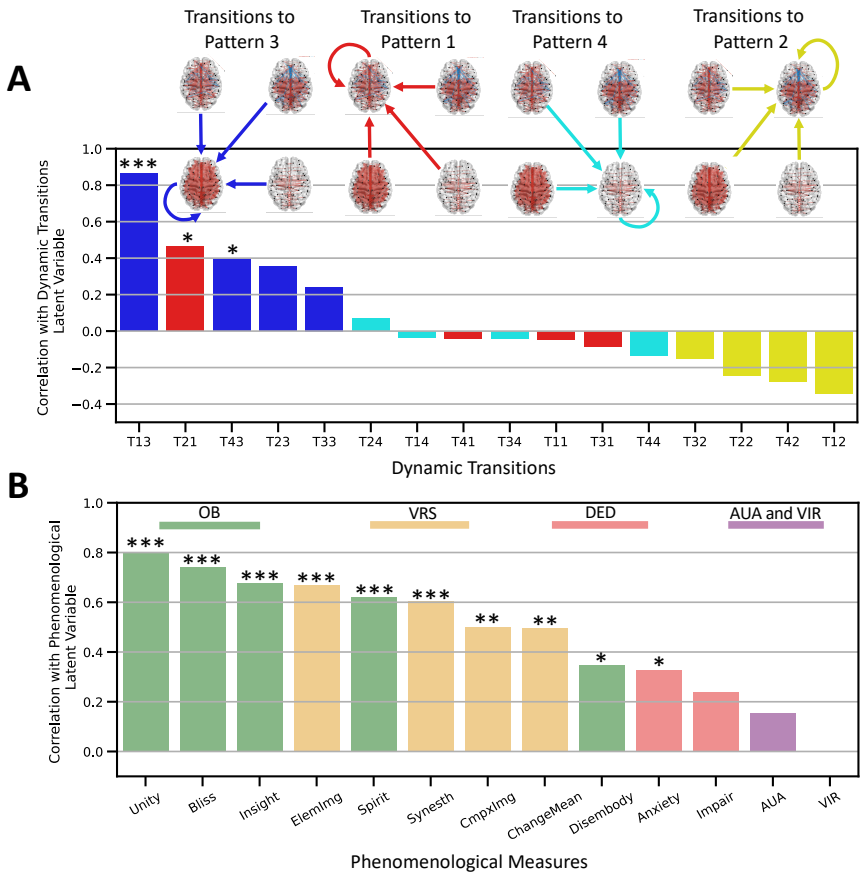

Figure 3. The neurophenomenological analysis indicated that transitions to the hyperconnected Pattern 3 were linked to the factors of oceanic boundlessness and visionary restructuralization. A) In the neural space, the canonical correlation analysis showed that the transition probabilities to the hyperconnected pattern had the highest correlation with the first canonical vector of the space. *Notes*: The y-axis represents pattern transitions, e.g. T13: transition from Pattern 1 to Patten 3. **B)** In the phenomenological space, factors related to the dimension of oceanic boundlessness and visionary restructuralization showed the highest correlation with the first canonical vector of the space. Bars represent correlation values of each factor to the first canonical vector of its associated space. Asterisks represent correlation significance (*p<0.05, **p<0.01, ***p<0.001). *Notes:* Unity: experience of unity, Bliss: blissful state, Insight: insightfulness, Spirit: spiritual experience, Disembody: disembodiment, ElemImg: elementary imagery, Synesth: audio-

visual synesthesia, CmpxImg: complex imagery, ChangeMean: changed meaning of percept, Impair: Impaired control and cognition, AUA: auditory alterations, RIV: reduction of vigilance.

Table 1. There were substantial changes in subjective experience after psilocybin administration compared to placebo. Mann-Whitney U test results of comparison between 11-ASC factors of the *Psilocybin* and *Placebo* groups. rg = Glass rank biserial coefficient effect size.

		Psilocybin (n=21)		Placebo (n=26)		Stats (MW-U test)		
		mean	**SD**	**mean**	**SD**	**U**	**rg**	**p**
5D-ASC	Oceanic Boundlessness	35.09	23.58	3.78	5.56	528.5	.936	**< 0.001**
	Dread of Ego Dissolution	20.54	17.12	3.94	8.05	494	.81	**< 0.001**
	Visionary Restructuralization	42.97	19.20	5.33	9.23	528.5	.936	**< 0.01**
	Auditory Alterations	16.99	17.18	4.69	12.97	458.5	.679	**< 0.001**
	Vigilance Reduction	28.18	20.43	13.99	16.33	400.5	.467	**< 0.001**
11-ASC	Insightfulness	42.44	29.77	4.99	7.39	508	0.861	**<0.001**
	Spiritual Experience	21.73	22.04	3.33	6.91	435	0.593	**<0.001**
	Experience of Unity	33.27	30.57	2.85	4.70	483.5	0.771	**<0.001**
	Blissful State	35.65	27.02	4.36	7.04	489	0.791	**<0.001**
	Disembodiment	20.65	25.71	1.74	1.82	434	0.59	**<0.001**
	Anxiety	19.55	22.57	3.01	4.30	430	0.575	**<0.001**
	Impaired Control and Cognition	24.29	18.35	4.77	12.51	497	0.821	**<0.001**
	Changed Meaning of Percept	36.75	29.65	4.24	8.92	495.5	0.815	**<0.001**
	Audio-Visual Synesthesia	49.54	22.82	4.94	12.99	525	0.923	**<0.001**
	Complex Imagery	36.43	25.49	6.22	12.03	528.5	0.839	**<0.001**
	Elementary Imagery	49.25	21.95	5.68	9.24	502	0.943	**<0.001**

Table 2. The neurophenomenological analysis indicated that transitions from Pattern 1 to the hyperconnected Pattern 3 were linked to Oceanic Boundlessness. Canonical correlation analysis between between-state transition probabilities and five dimensions of the 5D-ASC. The results are sorted from the highest correlation to the lowest.

	Factor	Correlation Coefficient	p-value	p-value (FDR-Corrected)
Neural Space	T13	0.89	1.54e-15	2.46e-14 ***
	T23	0.44	3.66e-03	2.33e-02 *
	T43	0.43	4.38e-03	2.33e-02 *
	T33	0.25	1.12e-01	2.25e-01
	T21	0.23	1.52e-01	2.69e-01
	T14	0.12	4.36e-01	6.34e-01
	T32	0.09	5.65e-01	6.67e-01
	T24	0.09	5.89e-01	6.67e-01
	T31	-0.01	9.41e-01	9.41e-01
	T44	-0.08	6.26e-01	6.67e-01
	T11	-0.09	5.63e-01	6.67e-01
	T41	-0.17	2.92e-01	4.67e-01
	T34	-0.27	7.86e-02	1.80e-01
	T22	-0.33	3.13e-02	8.34e-02
	T12	-0.34	2.93e-02	8.34e-02
	T42	-0.34	2.85e-02	8.34e-02
Phenomenological Space	OBN	0.93	1.51e-19	7.55e-19 ***
	VRS	0.74	1.95e-08	4.89e-08 ***
	DED	0.46	1.94e-03	3.24e-03 **
	AUA	0.35	2.46e-02	3.08e-02 *
	VIR	0.11	4.92e-01	4.92e-01

Tij: probability of transition from Pattern i to Pattern j. OBN: oceanic boundlessness, VRS: visionary restructuralization, DED: dread of ego dissolution, AUA: auditory alteration, VIR: vigilance reduction.

626